

UC Davis

UC Davis Previously Published Works

Title

Rapid Throughput Analysis of GABAA Receptor Subtype Modulators and Blockers Using DiSBAC1(3) Membrane Potential Red Dye

Permalink

<https://escholarship.org/uc/item/38t8s6k5>

Journal

Molecular Pharmacology, 92(1)

ISSN

0026-895X

Authors

Nik, Atefeh Mousavi
Pressly, Brandon
Singh, Vikrant
[et al.](#)

Publication Date

2017-07-01

DOI

10.1124/mol.117.108563

Peer reviewed

Mol #108563

TITLE PAGE

Rapid Throughput Analysis of GABA_A Receptor Subtype Modulators and Blockers Using DiSBAC₁(3) Membrane Potential Red Dye

Atefeh Mousavi Nik, Brandon Pressly, Vikrant Singh, Shane Antrobus, Susan Hulsizer, Michael A. Rogawski, Heike Wulff and Isaac N. Pessah

Department of Molecular Biosciences, School of Veterinary Medicine (A.M.N., S.A., S.H., I.N.P.); Department of Pharmacology (B.P., V.S., M.A.R., H.W.), School of Medicine, University of California, Davis, Davis, CA 95616, USA; and Department of Neurology (M.A.R.), School of Medicine, University of California, Davis, Sacramento, CA 95817; The Medical Investigation of Neurodevelopmental Disorders (MIND) Institute (I.N.P.), Sacramento, CA 95817, USA

Mol #108563

RUNNING TITLE PAGE

Running title:

Analysis of GABA_A receptor modulators with potentiometric dye

Corresponding author:

Isaac N. Pessah, Department of Molecular Biosciences, School of Veterinary Medicine, University of California, Davis, One Shields Avenue, Davis, CA 95616, USA. Phone: (530) 752-6696; E-mail: inpessah@ucdavis.edu

Number of text pages: 20

Number of tables: 2

Number of figures: 10

Number of Supplemental Figures: 3

Number of references: 46

Number of words in *Abstract*: 251

Number of words in *Introduction*: 792

Number of words in *Discussion*: 1226

List of nonstandard abbreviations:

AFU, arbitrary fluorescence unit; Ara-C, cytosine arabinoside; BDZ, benzodiazepine; DiSBAC₁(3), 5,5'-(1-propen-1-yl-3-ylidene)bis[1,3-dimethyl-2-thio-barbituric acid]; DZP, diazepam; E_m, equilibrium membrane potential; FLIPR[®], Fluorometric Imaging Plate Reader; FMP-Red-Dye, FLIPR membrane potential red dye; GABA, γ -aminobutyric acid; GABA_AR, GABA_A receptor; HRMS, high-resolution mass spectrometry; MDZ, midazolam; NAS, neuroactive steroid; PAM, positive allosteric modulator; PTX, picrotoxin; 5 β ,3 α -THDOC, 3 α ,21-dihydroxy-5 β -pregnan-20-one; TBPS, *t*-butylbicyclophosphorothionate; TETS, tetramethylenedisulfotetramine; SAR, structure-activity relationship; XJ-42, (3 α ,5 α ,20E)-3-hydroxy-13,24-cyclo-18-norcholan-20-ene-21-carbonitrile

ABSTRACT

Fluorometric Imaging Plate Reader (FLIPR[®]) membrane potential dye (FMP-Red-Dye) is a proprietary tool for basic discovery and high throughput drug screening for G-protein coupled receptors and ion channels. We optimized and validated this potentiometric probe to assay functional modulators of heterologous expressed GABA_A receptor (GABA_AR) isoforms (synaptic $\alpha 1\beta 3\gamma 2$, extrasynaptic $\alpha 4\beta 3\delta$, and $\beta 3$ homopentomers). High-resolution mass spectrometry identified FMP-Red-dye as DisSBAC₁(3). GABA_AR expressing cells equilibrated with FMP-Red-Dye exhibited depolarized equilibrium membrane (E_m) potentials compared to GABA_AR-null cells. The channel blockers picrotoxin, fipronil, tetramethylenedisulfotetramine (TETS), and the competitive antagonist bicuculline reduced fluorescence near the levels in GABA_AR-null cells indicating that FMR-Red-Dye, a barbiturate derivative, activates GABA_AR-mediated outward Cl⁻ current in the absence of GABA. GABA caused concentration-dependent increases in fluorescence with rank order of potencies among GABA_AR isoforms consistent with results from voltage-clamp experiments (EC_{50} values for $\alpha 4\beta 3\delta$, $\alpha 1\beta 3\gamma 2$, $\beta 3$ homopentamers were 6 ± 1 nM, 40 ± 11 nM, >18 mM) respectively, whereas GABA_AR-null cells were unresponsive. Neuroactive steroids (NAS) increased fluorescence of GABA_AR expressing cells in the absence of GABA and demonstrated positive allosteric modulation (PAM) in the presence of GABA, whereas benzodiazepines only exhibited PAM activity. Of 20 NAS tested, allopregnanolone, (3 α ,5 α ,20E)-3-hydroxy-13,24-cyclo-18-norcholane-20-ene-21-carbonitrile (XJ-42), eltanolone, 5 β -pregnan-3 α ,21-diol-20-one, and ganaxolone showed the highest potency. The FMP-Red-Dye-based assay described here provides a sensitive and quantitative method of assessing the activity of GABA_AR agonists, antagonists and PAMs on diverse GABA_AR isoforms. The assay has a wide range of applications, including screening for antiseizure agents and identifying channel blockers of interest to insecticide discovery or biosecurity.

INTRODUCTION

GABA_A receptors (GABA_AR) are ligand-gated anion channels that mediate inhibition in the mammalian central nervous system by responding to the neurotransmitter γ -aminobutyric acid (GABA) (Barnard et al., 1998). GABA_AR dysfunctions are associated with epilepsy, autism, fragile X syndrome, depression and schizophrenia (Braat and Kooy, 2015; Rudolph and Möhler, 2014; Stafstrom et al., 2012; Verkman and Galietta, 2009). GABA_AR are also the primary toxicological targets of several current use insecticides (e.g., fipronil) and pesticides of historical importance that persist in the environment (e.g., organochlorines) (Casida and Durkin, 2015). Importantly, GABA_AR are a major pharmacological target for antiseizure drugs (Brodie et al., 2016).

GABA_AR are pentameric anion channels composed of two α subunits, two β subunits and one subunit, which is designated γ , δ , ϵ , θ , or π . There are multiple isoforms of many of the subunits, six for α , three for β , and three for γ , allowing for a high degree of variation depending on brain region and developmental stage. Most synaptic GABA_AR contain two α , two β subunits and one γ 2 subunit, have a relatively low affinity for GABA and mediate fast phasic inhibition (Brickley and Mody, 2012; Rissman and Mobley, 2011). In contrast, extrasynaptic GABA_AR often contain a δ subunit, have a higher affinity for GABA and mediate persistent tonic inhibition (Belelli et al., 2009; Bettler and Tiao, 2006; Brickley and Mody, 2012). In addition to the endogenous neurotransmitter, GABA, which binds to the interface of α and β subunits, GABA_AR possess binding sites for neuroactive steroids (NAS), benzodiazepines, and barbiturates that allosterically enhance GABA-activated Cl⁻ conductance and in some instances activate Cl⁻ conductance in the absence of GABA, thereby exerting anxiolytic, sedative, and antiseizure effects that are useful for treating anxiety and sleep disorders, epilepsy, as well as

Mol #108563

serving as general anesthetics (Belelli et al., 2009; Belelli and Lambert, 2005; Herd et al., 2007). The benzodiazepine binding site is localized between the α and γ subunits, whereas NAS are known to have two binding sites, a potentiation site on the α subunit and a direct activator site in the α/β interface, both of which need to be occupied for potent channel activation (Akabas, 2004; Alvarez and Estrin, 2015; Campagna-Slater and Weaver, 2007; Hosie et al., 2007). Although the precise site(s) to which barbiturates bind remain elusive, domains within β subunit transmembrane segments TM2 and TM3 appear to be critical (Loscher and Rogawski, 2012). Interestingly, $\beta 3$ subunits reconstitute a homopentameric channel that possesses NAS binding sites (Chen et al., 2012; Miller and Aricescu, 2014; Alvarez and Estrin, 2015).

Considering the utility of GABA_AR as therapeutic targets, there is substantial interest in the identification of improved GABA_AR modulators. A suitable high-throughput screening method would significantly aid in the identification of such agents. One potential method to assess GABA_AR function in a high-throughput manner uses the Fluorometric Imaging Plate Reader (FLIPR) membrane potential dye FMP-Red-Dye that redistributes across the plasma membrane in a voltage-dependent manner. Cell depolarization results in dye movement into the cell and binding to intracellular proteins and hydrophobic sites causing increased fluorescence signals and vice-versa occurs for hyperpolarization. Thus, FMP-Red-Dye allows monitoring of membrane potential changes in a bidirectional fashion independent of ion type. FMP-Red-Dye is convenient in that it does not require cells to be washed of excess dye after equilibration due to inclusion of a proprietary cell membrane impermeant red wavelength quencher, which results in a high signal-to-noise ratio (Fairless et al., 2013). Mennerick et al. reported that many voltage-sensitive dyes such as Di-4-ANEPPS and DiBAC₄(3) can directly activate and/or potentiate GABA_AR currents in a manner similar to NAS and barbiturates (Mennerick et al., 2010), questioning their usefulness for screening GABA_AR ligands. A previous study reported that

Mol #108563

FMP-Red-Dye had a better performance than FMP-Blue-Dye, and that it produced results comparable to electrophysiology (Joesch et al., 2008). However, the chemical identity of FMP-Red-Dye is proprietary and the degree to which its constituents might influence GABA_AR function and therefore limit the dye's usefulness in characterizing GABA_AR modulators has remained unclear.

Here we identify the voltage-sensitive component of FMP-Red-Dye as DiSBAC₁(3), optimize and validate its use as a rapid throughput indicator of GABA_AR activators, blockers and PAMs using FLIPR, and implement the assay to screen a small library of NAS and channel blockers. We show that FMP-Red-Dye can be used to differentiate GABA_AR mediated responses in cell lines that stably or transiently express synaptic ($\alpha 1\beta 3\gamma 2$), extrasynaptic ($\alpha 4\beta 3\delta$), or $\beta 3$ homomeric GABA_AR isoforms. We conclude that the FMP-Red-Dye based assays provide sensitive and quantitative approaches to investigate functional drug effects on GABA_AR isoforms, whether they are mediated by binding to the GABA recognition site, the NAS PAM sites, or convulsant channel blocking sites. The assay is useful for antiseizure drug screening and identifying novel channel blockers of interest to insecticide discovery or biosecurity.

MATERIALS AND METHODS

Reagents

Poly-L-lysine, cytosine arabinoside (Ara-C), picrotoxin (PTX), *t*-butylbicyclophosphorothionate (TBPS), fipronil, bicuculline, diazepam and γ -aminobutyric acid (GABA) were purchased from Sigma Aldrich (St. Louis, MO). Falcon™ 96-Well Imaging Plates with Lid were purchased from Fisher Scientific (Hampton, NH). FLIPR Membrane Potential Red Assay Kit (FMP-Red-Dye; Part number: R8123) was purchased from Molecular Devices Corporation (Sunnyvale, CA). Fluo4-AM was purchased from Life Technology (Hampton, NH).

Mol #108563

GS21 supplement (Cat# GSM-3100) was purchased from MTI-Global stem (Gaithersburg, MD). Org 20599, alphaxalone, eltanolone, progesterone and midazolam were purchased from Tocris (Pittsburgh, PA). (3 α ,5 α ,20E)-3-hydroxy-13,24-cyclo-18-norcholestan-20-ene-21-carbonitrile (XJ-42; Compound 63 in Covey and Jiang, 2014) was a generous gift of Dr. Douglas F. Covey (Washington University School of Medicine, St. Louis, MO), 3-[3 α -hydroxy-3 β -methyl-5 α -androstane-17 β -yl]-5-(hydroxymethyl)isoxazole (UCI-50027; Hogenkamp et al., 2014) was a generous gift of Dr. Kelvin W. Gee (University of California, Irvine, Irvine CA). Allopregnanolone was custom synthesized by SAFC Pharma (Madison, WI). Dehydroepiandrosterone sulfate, indiplon, and ursodeoxycholic acid (sodium salt) were purchased from Cayman Chemical (Ann Arbor, MI). Dehydroepiandrosterone acetate, dehydroepiandrosterone, cortisol, epiandrosterone, 20 α -dihydropregnenolone, androstenediol, etiocholanolone, androsterone, alphadolone 21-acetate and tetrahydrocortexone were purchased from Steraloids (Newport, RI). Tetramethylenedisulfotetramine (TETS) was synthesized in the laboratory of Dr. Bruce Hammock as previously described (Zhao et al., 2014). All reagents were >97% purity.

Heterologous Expression of GABA_AR Isoforms

Expression of GABA_AR subunits for potentiometric measurements with FLIPR FMP-Red-Dye

Our goal was to develop a reliable, rapid throughput approach to quantitatively assess the influences of blockers, antagonists, and PAMs on the functional activity of diverse GABA_AR isoforms. To this end, we investigated cell lines that stably or transiently express three GABA_AR isoforms of different subunit compositions. A HEK 293 (human embryonic kidney) cell line that stably expresses human GABA_AR α 1 β 3 γ 2 subunits (CYL3053 PrecisION hGABA-A α 1/ β 3/ γ 2-HEK Recombinant Cell Line) was a generous gift of EMD Millipore Corporation, St. Charles,

Mol #108563

MO. GABA_AR $\alpha_1\beta_3\gamma_2$ heteropentameric channels primarily localize to synaptic sites in mammalian neurons (McCartney et al., 2007). The GABA_AR-null HEK 293 line, which served as control, was purchased from American Type Culture Collection (ATCC-CRL-1573). Upon arrival both cell lines were expanded in Dulbecco's modified Eagle's medium/Ham's F-12 (50/50 mix), 10% fetal bovine serum (FBS), 1% non-essential amino acid (Invitrogen, Carlsbad, CA) at 37°C in 5% CO₂ and several bullets frozen to limit passage numbers. Cells expressing $\alpha_1\beta_3\gamma_2$ subunits were kept under selection pressure with 400 $\mu\text{g}/\text{mL}$ gentamicin, 100 $\mu\text{g}/\text{mL}$ hygromycin B (Invitrogen) and 0.625 $\mu\text{g}/\text{mL}$ puromycin (Clontech). GABA_AR null cells were cultured in 100 U/mL penicillin and 100 $\mu\text{g}/\text{mL}$ streptomycin (Gibco) to minimize the risk of bacterial contamination. Cell lines were discarded after 15 passages. Cells were passaged when 70-80% confluent and harvested using 0.05% trypsin-EDTA and 50,000-60,000 cells/well (in a volume of 100 μl), seeded into poly-L-lysine-coated wells of a 96-well plate, and allowed to recover in the incubator overnight before FMP-Red-Dye loading and measurements of E_m with FLIPR.

A L-tk (mouse connective tissue) cell line expressing the human GABA_AR $\alpha_4\beta_3\delta$ subunit combination under a dexamethasone inducible promoter was kindly provided by Dr. Trevor Smart (University College, London) (Brown et al., 2002). The $\alpha_4\beta_3\delta$ subunit isoform is found at extrasynaptic sites in mammalian brain. The L-tk cell line was cultured in Dulbecco's MEM plus glutamine, 4.5 g/L Na pyruvate and glucose with 10% FBS, in the presence of 1 mg/mL gentamicin and 0.2 mg/mL zeocin to select $\alpha_4\beta_3\delta$ positive cells. Dexamethasone (1 μM ; Invitrogen) or vehicle was added to the media to induce $\alpha_4\beta_3\delta$ subunit expression or serve as GABA_AR-null cells, respectively, when 80-90% confluent. Cells were induced for 48 hrs, passaged using trypsin-EDTA 0.05%, and plated at 50,000-60,000 cells/well into 96 wells plates, and after 24 hrs recovery loaded with FMP-Red-Dye and membrane potential measured as described below.

Mol #108563

Transient expression of GABA_AR β_3 homopentamers in HEK 293 cells (ATCC CRL-1573) was achieved with a pcDNA3.1 expression vector generously provided by Dr. Robert L. Macdonald (Vanderbilt University, Nashville, TN). HEK 293 cells were cultured as described above. Twenty-four hours before transfection, cells were plated on 10-cm tissue culture treated dishes and transfected with plasmid DNA at 70%-90% confluence using TurboFect (Thermo Scientific) according to manufacturer's instruction. At 24 hrs post-transfection, cells were dissociated with trypsin, counted and plated on poly-L-lysine coated 96-well plates (Falcon) at a density of 50,000-60,000 cells/well. All FLIPR experiments were carried out 48 hrs post transfection.

Expression of GABA_AR subunits for electrophysiological measurements

The human GABA_AR α_1 , β_3 and γ_2 cloned into pcDNA3.1 expression vectors were a gift from Dr. Robert L. Macdonald, Vanderbilt University, TN. Fibroblast L929 cells were cultured in Dulbecco's modified Eagle's medium (Lonza) supplemented with 10% fetal bovine serum, 100 U/mL penicillin and 100 mg/mL streptomycin (Invitrogen) and maintained in humidified 95% air and 5% CO₂ air at 37°C. Cells were transfected using FuGENE 6 (Roche) transfection reagent with an equal amount of each of the subunits in combination with pEGFP-C1. The transfection ratio of total cDNA to transfection reagent was 2:1 with equal amounts of α_1 , β_3 , γ_2 cDNA to reconstitute synaptic $\alpha_1\beta_3\gamma_2$ GABA_AR, or β_3 alone to reconstitute homopentamers. Two days post-transfection, cells were plated on glass coverslips and transfected cells were identified using an epifluorescence microscope for electrophysiological measurements. Electrophysiological recordings from L-tk cells expressing GABA_AR $\alpha_4\beta_3\delta$ subunit composition were obtained with culture and induction methods described above.

Mol #108563

Rapid Throughput Analysis of GABA_AR Modulators Using FLIPR FMP-Red-Dye

Once HEK 293 and L-tk cells were cultured on 96-well plates for 24 hrs, FMP-Red-Dye was reconstituted to 1× with 100 ml of Locke's buffer (NaCl 154 mM, KCl 5.6 mM, CaCl₂ 2.3 mM, MgCl₂ 1 mM, HEPES 8.6 mM, glucose 5.6 mM, glycine 0.1 μM, pH 7.4) as recommended by the supplier (Molecular Devices). Growth media was removed from the wells and cells were loaded with 100 μl FMP-Red-Dye solution for 30 min in the dark at room temperature (except for experiments in Fig. 1 where fluorescence signals were recorded immediately). Each plate was transferred to the FLIPR Tetra Station and the dye excited at 510–545 nm, and the fluorescent signals recorded at 565–625 nm. Baseline recording were acquired for 2 min at a sampling rate of 1 Hz (400 ms of illumination per sample). FMP-Red-Dye is a slow-response potential-sensitive probe and the maximal response is usually seen within 2 min after triggering cellular depolarization or hyperpolarization (see Figures 3 and 4; (Dasheiff, 1985)). Cell responses were normalized by calculation $(F_{\max} - F_{\min})/F_{\min} = \Delta F/F_0$, where F_{\max} was the maximum response in arbitrary fluorescence units (AFU), and F_{\min} was the baseline AFU value.

Although HEK 293 cells were unresponsive to vehicle additions, signals from L-tk cells expressing $\alpha_4\beta_3\delta$ subunits exhibited an abrupt but transient drop in fluorescence with addition of any solution, including Locke's or vehicle, and therefore, all data from L-tk cells were normalized to vehicle baseline by subtraction.

Electrophysiological Recordings

Whole-cell voltage-clamp and current-clamp recordings were performed at room temperature with an EPC-10 HEKA amplifier. Cells were bathed in an external Ringer solution consisting of 160 mM NaCl, 4.5 mM KCl, 1 mM MgCl₂, 2 mM CaCl₂, 10 mM HEPES, pH 7.4, 311 mOsm. Recording electrodes were pulled and fire-polished to resistances of 1.8-2.4 MΩ for voltage-clamp and 3-6 MΩ for current-clamp experiments. Electrodes were filled with an

Mol #108563

internal solution consisting of 154 mM KCl, 2 mM CaCl₂, 1 mM MgCl₂, 10 mM HEPES and 10 mM EGTA with pH 7.3 and 308 mOsm. Cells were voltage clamped at -80 mV and control currents were recorded under the application of 1 μM GABA, using a gravity-fed fast perfusion system, for 5 s followed by a 40-50 s wash with external solution. GABA concentration-response relationships were determined by testing increasing concentrations of GABA and normalizing GABA currents to the peak response induced by a saturating concentration of GABA. Normalized currents were fitted using the Hill equation to determine the EC₅₀ and EC₁₀ values. The EC₁₀ (1 μM) was used to evaluate the positive modulatory effects of the neurosteroids. The increases in Cl⁻ current elicited in the presence of NAS were compared to the initial EC₁₀ to determine the fold increase in current. Test solutions of the NAS were freshly prepared immediately before each application onto cells. Membrane potential was recorded on the initial break into the cell while in current-clamp mode. For experiments involving FMP-Red-Dye, cells were pre-incubation with the dye for 30 min before recording in the absence or presence of fipronil. Cells were then exposed to 10 min of UV irradiation (460-490 nm) to induce the previously reported photodynamic effect of voltage-sensitive dyes (Mennerick et al., 2010).

Data Analysis

GraphPad Prism software (Version 6) was used for statistical analysis and graphing. EC₅₀ values were determined using nonlinear regression with a four-parameter logistic equation. Student's *t*-test or F test (P<0.05) was applied to determine statistical differences. For post-hoc multiple comparison separate one-way ANOVA (for EC₅₀ and slope) using Tukey test was applied. Data are presented as the mean ± S.D. as stated. For electrophysiology, data analysis was performed using Excel (Microsoft) and Origin 7.0 (OriginLab Corp.) software. Data fitting

Mol #108563

to the Hill equation to obtain EC₅₀ values was performed with Origin 7.0. Data are presented as the mean ± S.D.

RESULTS

Optimization and Evaluation of FMP-Red-Dye Assay for Functional GABA_AR Screening

In initial experiments, HEK 293 cells stably expressing one of the widely expressed human synaptic GABA_AR isoforms $\alpha 1\beta 3\gamma 2$ or GABA_AR-null HEK 293 cells were used to test whether FMP-Red-Dye potentiates GABA_AR function in the absence of GABA as reported for other potentiometric dyes (Mennerick et al., 2010). FMP-Red-Dye signals were monitored in real-time within 1 min after dye addition to the cell medium. Initial fluorescence signals were similar for both GABA_AR-expressing and GABA_AR-null HEK 293 cells, but equilibrated to different steady-state fluorescence signals within 30 minutes, with $\alpha 1\beta 3\gamma 2$ -expressing HEK 293 cells invariably achieving 2-fold higher steady-state fluorescence intensity than the respective null cells (**Fig. 1A**). Importantly, inclusion of PTX (1 μ M) with dye addition prevented the rise in fluorescence in GABA_AR-expressing cells (**Fig. 1A**). In contrast, inclusion of GABA (1 μ M) with the potentiometric dye caused an instantaneous increase in dye signal (within the 1 Hz resolution of the recording) followed by a more gradual equilibration of fluorescence to a 3-fold greater signal than that achieved in null cells by 30 min (**Fig. 1C**). GABA_AR-null cells showed a minimal time-dependent fluctuation in fluorescence and this response was unchanged by the presence of GABA. Similar results were obtained in studies comparing FMP-Red-Dye responses in L-tk cells expressing the extrasynaptic $\alpha 4\beta 3\delta$ GABA_AR isoform with L-tk GABA_AR-null cells (**Fig. 1B and 1D**). These results indicate that by itself FMP-Red-Dye promotes slow depolarization of cells expressing either synaptic or extrasynaptic GABA_AR subunits but fails to cause this effect in the respective null cells. FMP-Red-Dye-induced cell depolarization was

Mol #108563

prevented by PTX indicating that it requires functional GABA_A receptors. In contrast to the apparent slow activation of GABA_AR caused by FMP-Red-Dye, GABA induced a rapid activation of the receptors.

To further verify the accuracy of our interpretation, FMP-Red-Dye was equilibrated for 30 min with $\alpha 1\beta 3\gamma 2$ -expressing or GABA_AR-null HEK 293 cells and membrane potential recorded in the current clamp mode of the patch-clamp technique. While null HEK cells had a resting membrane potential of -78.6 ± 6.3 mV, which did not significantly change after incubation with FMP-Red-Dye (**Fig. 2**), $\alpha 1\beta 3\gamma 2$ expressing HEK 293 cells had a more positive resting membrane potential of -68.8 ± 6.6 mV ($P = 0.02$), which was depolarized by a further 9 mV to -59.6 ± 6.9 mV ($P = 0.03$) after incubation with FMP-Red-Dye for 30 min. This depolarization could be prevented by the GABA_AR blocker fipronil (**Fig. 2**). Interestingly, 10 min of UV irradiation (460-490 nm) induced the previously reported photodynamic effect of voltage-sensitive dyes (Mennerick et al., 2010), and induced a further depolarization of the $\alpha 1\beta 3\gamma 2$ expressing HEK cells to -42.8 ± 10.1 mV ($P = 0.002$) (**Fig. 2**).

The light-dependent influences of FMP-Red-Dye on cells expressing GABA_AR isoforms compelled us to determine its chemical identity, which to date has been proprietary information. The excitation and emission characteristics of the red dye (Ex 470 / Em 580 nm) suggest that the dye is a member of one of two structurally related families of voltage-sensitive dyes, DiBAC and/or DiSBAC. These dyes, which are derivatives of barbituric or thiobarbituric acid (Supplemental **Fig. 1A**), may bind at the barbiturate binding sites of GABA_AR (Mennerick et al., 2010). High-resolution mass spectrometry (HRMS) was used to elucidate the molecular identity of FMP-Red-Dye in its complex matrix. An experimental molecular mass of 379.0521 was obtained (Supplemental **Fig. 1B**), which is within 5 ppm of the theoretical molecular mass of

Mol #108563

379.0534 of the voltage-sensitive dye 5,5'-(1-propen-1-yl-3-ylidene)bis[1,3-dimethyl-2-thio-barbituric acid (DiSBAC₁(3); CID 53485318).

Collectively these results, suggested that under tightly controlled experimental conditions the FMP-Red-Dye FLIPR platform could provide a sensitive and quantitative method for investigating pharmacological responses of GABA_AR isoforms to diverse direct GABA_AR activators, GABA_AR channel blockers of toxicological significance, and GABA_AR PAMs. To these ends, subsequent experiments were conducted following 30 min equilibration of cells seeded in 96-well plates with dye in the dark, followed by 2 min of baseline recording and 10 min of response recording after drug addition from a 96-well source plate. Excitation and emission were within visible wavelengths (ex 510–545 nm/em 565–625 nm) wells were excited by 400 ms duration pulsed illumination at a rate of 1 Hz. This protocol minimizes photodynamic influences of the FMP-Red-Dye, which may alter its activity on GABA_AR.

Differential Potencies of GABA Toward Activating Synaptic and Extrasynaptic GABA_AR

Concentration-response relationships for GABA were obtained using the FMP-Red-Dye assay in heterologous cells expressing either the synaptic GABA_AR isoform $\alpha 1\beta 3\gamma 2$ or the extrasynaptic isoform $\alpha 4\beta 3\delta$. Figure 3A shows representative responses to a range of GABA concentrations from 0.1 nM to 30 μ M. The respective GABA_AR-null HEK 293 or L-tk cells, in contrast, did not respond to GABA. The concentration-response curves in Fig. 3B, left indicate that GABA was significantly more potent at eliciting a fluorescence signal in cells expressing $\alpha 4\beta 3\delta$ than in cells expressing $\alpha 1\beta 3\gamma 2$ (EC₅₀ values, 6 ± 1 nM, 95% CI: 4-16 nM and 40 ± 11 nM, 95% CI: 30-53 nM, respectively). HEK 293 cells expressing homopentameric $\beta 3$ subunits were largely insensitive to GABA at concentrations ≤ 1 mM, although these cells did exhibit

Mol #108563

fluorescence responses to higher concentrations of GABA that were sensitive to PTX (see **Fig. 5**).

Voltage-clamp experiments performed with cells expressing the same subunit compositions used in the FMP-Red-Dye experiments confirmed that the cells expressing $\alpha 4\beta 3\delta$ GABA_AR were more sensitive to GABA than those expressing $\alpha 1\beta 3\gamma 2$ subunits ($P < 0.05$; **Fig. 3B, right**). Comparing results using the two approaches indicated that the FMP-Red-Dye assay was a very sensitive measurement of GABA-triggered depolarization. Regardless, with both experimental approaches $\alpha 4\beta 3\delta$ was more sensitive to GABA than $\alpha 1\beta 3\gamma 2$ (7-fold for FMP-Red-Dye assay and 12-fold for the patch-clamp technique).

Whether FMP-Red-Dye itself was directly responsible for the greater sensitivity to GABA obtained with the fluorescence assay than with the voltage-clamp assay was assessed by repeating the fluorescence experiments with a 2-fold dilution of dye in HEK 293 cells expressing $\alpha 1\beta 3\gamma 2$ (**Fig. 3, inset**). Under these conditions, the GABA concentration-effect relationship was shifted to the right such that the EC₅₀ value (500 nM) was approximately 10-fold higher than with the FMP-Red-Dye dilutions recommended by the supplier (EC₅₀, 40 nM). These results suggest that FMP-Red-Dye acting as a PAM enhances the GABA sensitivity of the fluorescence assay. We found that the 2-fold dilution reduced signal-to-noise and dynamic range and that the assay became unreliable with 5-fold dilution. We therefore routinely used FMP-Red-Dye at the dilution recommended by the supplier.

Differential Potencies of Blockers in Cells Expressing Different GABA_AR Isoforms

PTX and TETS are seizure-triggering toxicants that inhibit GABA_AR Cl⁻ current by binding to overlapping sites within the ion conducting pore of the channel (Adelsberger et al., 1998; Cao et al., 2012; Olsen, 2006). We sought to demonstrate that the FMP-Red-Dye assay can

Mol #108563

be used to assess the blocking activity of such agents in order to validate the assay as a means of identifying novel blockers and quantifying their activity in diverse GABA_AR isoforms. Both PTX and TETS reduced the FMP-Red-Dye signal in HEK 293 cells expressing the $\alpha 1\beta 3\gamma 2$ subunit combination in a concentration-dependent manner, but had negligible influence on GABA_AR-null cells (**Fig. 4; Table 1**). TETS was slightly more potent than PTX (IC₅₀ values, $3.8 \pm 1.1 \mu\text{M}$ and $6.5 \pm 1.5 \mu\text{M}$, respectively; $P < 0.0001$). Two additional allosteric blockers were tested, TBPS and the insecticide fipronil, and shown to have similar potencies to that of TETS (IC₅₀ values, 1.8 ± 1.2 and $2.6 \pm 1.1 \mu\text{M}$, respectively). The GABA_AR competitive antagonist bicuculline was approximately 20-times more potent than TBPS (IC₅₀ value, $0.1 \pm 0.1 \mu\text{M}$; $P < 0.0001$), although its efficacy at reducing fluorescence to that in GABA_AR-null cells was less complete at the highest concentration tested (10 μM , not shown).

L-tk cells expressing $\alpha 4\beta 3\delta$ subunits showed a distinct structure-activity relationship (SAR) with the blockers. Although the inhibitory potency of PTX was similar to that in cells expressing $\alpha 1\beta 3\gamma 2$ (IC₅₀ values, $6.0 \pm 1.0 \mu\text{M}$ vs. $6.5 \pm 1.5 \mu\text{M}$; $P > 0.31$), TETS was 2-fold less potent and TBPS and fipronil were nearly 200- and 10-fold more potent at the $\alpha 4\beta 3\delta$ isoform than at the $\alpha 1\beta 3\gamma 2$ isoform (**Table 1**).

The divergent potencies exhibited by inhibitors towards cells expressing different GABA_AR isoforms compelled us to determine responses of cells expressing only the $\beta 3$ subunit, which forms homopentamers that lack high-affinity GABA binding. HEK 293 cells expressing the $\beta 3$ homomeric isoform exhibited substantially greater fluorescence than the respective GABA_AR-null cells (**Fig. 5A**) as was the case for the $\alpha 1\beta 3\gamma 2$ isoform (**Fig. 4**), suggesting that FMP-Red-Dye is able to activate $\beta 3$ homomeric GABA_AR as it does the other isoforms. PTX caused a concentration-dependent inhibition of fluorescence (**Fig. 5C and D**) that brought the fluorescence near that in GABA_AR-null cells. $\beta 3$ -expressing cells failed to respond to GABA at

Mol #108563

concentrations below 1 mM (**Fig. 5B**), but as in previous voltage-clamp studies (Wooltorton et al., 1997) they did appear to be activated by high (>10 mM) GABA concentrations. **Figure 6A** showed that hyperpolarization produced by fipronil was also concentration dependent with fipronil being approximately 10- and 50-fold more potent at restoring E_m to levels near those measured with GABA_AR-null HEK 293 cells than PTX or TETS (**Table 1**).

Detection of Direct Activation and PAM Activity in GABA_AR Isoforms

Neuroactive steroids (NAS) have been shown to have GABA_AR PAM activity at low concentrations and to directly activate GABA_AR at higher concentrations (Belelli and Lambert, 2005; Wang, 2011). Twenty NAS and related structures were tested for activity on GABA_AR in the FMP-Red-Dye assay with heterologous cells expressing $\alpha 1\beta 3\gamma 2$, $\alpha 4\beta 3\delta$ or $\beta 3$ homomeric isoforms, and the potency and efficacy of active compounds quantified (**Figs. 7 and 8; Table 2**). Several NAS caused concentration-dependent increases in fluorescence in cells expressing the $\alpha 1\beta 3\gamma 2$ and $\alpha 4\beta 3\delta$ isoforms with EC_{50} values below 1 μ M whereas the respective GABA_AR-null cells failed to respond to any NAS. The rank order of potencies (based on EC_{50} values) in cells expressing the $\alpha 1\beta 3\gamma 2$ isoform was: allopregnanolone ~ eltanolone ~ XJ-42 > ganaxolone ~ 5 β ,3 α -THDOC ~ alphaxalone > alphadolone 21-acetate >> andosterone. Of these, 5 β ,3 α -THDOC and alphadolone 21-acetate showed significantly ($P < 0.001$) lower efficacy (maximum $\Delta F/F_0$) than the other active NAS (**Table 2**). By contrast, cells expressing the $\alpha 4\beta 3\delta$ isoform showed a different rank order of potencies: eltanolone > allopregnanolone > ganaxolone ~ 5 β ,3 α -THDOC ~ XJ-42 ~ alphaxalone >> alphadolone 21-acetate > androsterone. XJ-42 exhibited significantly greater maximal efficacy in cells expressing $\alpha 4\beta 3\delta$ ($P < 0.007$) than the other active NAS whereas 5 β ,3 α -THDOC had significantly lower efficacy (**Fig 7E and 8E; Table 2**). Overall, with the exception of eltanolone, all active NAS were modestly more potent

Mol #108563

on $\alpha 1\beta 3\gamma 2$ than $\alpha 4\beta 3\delta$ ($P < 0.0038$). In contrast to other isoforms, $\beta 3$ homopentameric channels were insensitive to allopregnanolone (**Fig. 6B**) and in general to all NAS tested (not shown).

We next tested whether the FMP-Red-Dye assay is able to detect the PAM activity of NAS and exposed cells to a low, submaximal concentration of GABA (10 nM) without and with various concentrations of NAS. **Fig. 9A** plots the fold increase in fluorescence signal in HEK 293 cells expressing the $\alpha 1\beta 3\gamma 2$ isoform in the presence of allopregnanolone or ganaxolone compared to the signal elicited by GABA alone. The EC_{50} values for the two NAS are 1.7 ± 1.2 nM ($n_H = 1.49$) and 20 ± 13 nM ($n_H = 1.43$), respectively. Because $GABA_{A}R$ channel open probability increases and maximizes with increasing GABA concentrations, the relative increase in response by a PAM will necessarily drop in magnitude as the GABA concentration is increased. This is demonstrated in the experiment of Fig. S3. The relative enhancement produced by 1 nM allopregnanolone in the presence of 1, 10, and 100 nM GABA is greatest at the lowest GABA concentration, reduced at 10 nM GABA, and there is no further enhancement with 100 nM GABA, which is a near saturating GABA concentration in the FMP-Red-Dye assay (**Fig. 3B**). Results from voltage-clamp experiments demonstrating the PAM effect with transiently expressed $\alpha 1\beta 3\gamma 2$ $GABA_{A}R$ are shown in **Fig. 9B**. Addition of allopregnanolone or ganaxolone in the presence of the GABA EC_{10} values (1 μM , **Fig. 3B**) caused a concentration-dependent enhancement of the Cl^{-} current with EC_{50} values of 71.7 ± 14.2 nM ($n_H = 1.8$) and 114.8 ± 15.6 nM ($n_H = 2.2$), respectively.

Finally, we tested whether the FMP-Red-Dye assay could detect direct or PAM effects of the benzodiazepine midazolam (MDZ). In the absence of GABA, midazolam failed to substantially enhance the fluorescence signal in HEK 293 cells expressing the $\alpha 1\beta 3\gamma 2$ isoform at concentrations ≤ 1 μM although at higher concentrations a small signal was elicited (**Fig. 10**). In

Mol #108563

the presence of suboptimal GABA (10 nM), midazolam caused a concentration-dependent increase in fluorescence signal with EC₅₀ value of 51 ± 12 nM (**Fig. 10**).

DISCUSSION

The present results demonstrate that FMP-Red-Dye, which contains the fluorescent voltage-sensor DiSBAC₁(3), can be used with the FLIPR platform to characterize a wide range of GABA_AR blockers and modulators in heterologously expressed recombinant GABA_AR. However, because FMP-Red-Dye interacts with GABA_AR, causing a PAM effect, quantitative results obtained with the potentiometric dye approach may not correspond to results obtained with other methods, such as the gold standard voltage-clamp technique. The potentiometric indicator DiSBAC₁(3) is a thio-barbiturate. Compared to other potentiometric dyes in the family of oxonol slow indicators, DiSBAC indicators have been reported to have reduced direct activating and PAM influences on GABA_AR compared to BiBAC dyes (Mennerick et al., 2010). Our present data indicate that DiSBAC₁(3) is a relatively weak direct activator of GABA_AR-mediated Cl⁻ currents in the absence of GABA or UV irradiation, but as previously reported for oxonols, UV irradiation greatly potentiates this activity. Equilibration of HEK 293 or L-tk cells that express GABA_AR with FMP-Red-dye in the dark results in a modest chronic depolarization of resting E_m regardless of GABA_AR isoform expression compared to respective GABA_AR-null cells. Depolarization of cells expressing GABA_AR by FMP-Red-dye is likely the direct consequence of interactions of the dye molecules at barbiturate sites localized within membrane spanning regions of the β subunit to directly activate Cl⁻ current (Löscher and Rogawski, 2012). In the case of our HEK 293 or L-tk cell expression models, the electrochemical gradient for chloride causes an inward current (outward Cl⁻ flux) that results in depolarization when GABA_AR channel opening is increased and hyperpolarization when channel opening is decreased, consistent with voltage-clamp measurements here and those of others in such cell types. This interpretation is supported by the experimental findings with channel blockers,

Mol #108563

including PTX, TETS or fipronil, that bring the fluorescence signal back to levels near those measured in the respective GABA_AR-null cells.

It is noteworthy that in both the potentiometric and voltage-clamp assays, GABA was ~10-fold more potent as an activator of the extrasynaptic subunit combination $\alpha 4\beta 3\delta$ than of the synaptic subunit combination $\alpha 1\beta 3\gamma 2$, while $\beta 3$ homopentamers were insensitive to GABA (≤ 1 mM). These differences in GABA sensitivity are in accord with previous reports (Brickley and Mody, 2012; Mortensen et al., 2011). For both the synaptic and extrasynaptic subunit combinations, GABA potency in the FMP-Red-Dye assay was two orders of magnitude greater than in patch-clamp experiments. A review of the available electrophysiological literature indicates that conventional barbiturates, such as pentobarbital, induce a more modest 3- to 10-fold leftward shift in sensitivity to GABA (Löscher and Rogawski, 2012; Steinbach and Akk, 2001). The basis for the extreme GABA sensitivity in the FMP-Red-Dye assay is not fully understood but could relate to the fact that the DiSBAC₁(3) molecule contains two thiobarbiturate moieties, which could interact with multiple sites on GABA_A receptors thus acting as synergistic positive modulators. Whatever the cause of the high sensitivity to GABA, the FMP-Red-Dye FLIPR platform provides an extremely sensitive assay for detecting and quantifying responses to GABA_AR agonists, antagonists and modulators on defined GABA_AR subtypes.

Two new findings emerge from studies with the potentiometric assay. First, the rank order of potencies of noncompetitive GABA_AR blockers towards $\alpha 1\beta 3\gamma 2$ (TBPS>TETS~fipronil>PTX) differs from that of $\alpha 4\beta 3\delta$ (TBPS>>fipronil>>TETS~PTX). Second, the approximately 10- and 100-fold higher potencies of fipronil and TBPS towards blocking the basal activity (i.e, normalizing E_m in the absence of GABA) of cells expressing the extrasynaptic $\alpha 4\beta 3\delta$ combination compared to either those that express the synaptic $\alpha 1\beta 3\gamma 2$ combination or $\beta 3$ homopentamers is particularly noteworthy in that it suggests for the first time that blockers with both compact and elongated chemical structures (Zhao et al.,

Mol #108563

2014) selectively target major extrasynaptic GABA_AR within the mammalian central nervous system, albeit with TBPS having 25-fold higher potency than fipronil (see **Table 1**). We also note that fipronil is substantially more potent than either PTX or TETS (10-fold and 50-fold, respectively) towards $\beta 3$ homopentamers, as previously demonstrated in receptor binding studies (Chen et al., 2006; Zhao et al., 2014). The findings identifying differential potencies of blockers towards synaptic and extrasynaptic GABA_AR subunit combinations could help explain outstanding questions with respect to toxicological mechanisms, including the pharmacodynamic basis for the different seizure-inducing potencies of different GABA_AR blockers. In addition, if it is the case that TBPS and fipronil are generally more active at extrasynaptic GABA_AR subunit combinations, these agents may be useful as pharmacological tools for selectively blocking these receptors. The competitive GABA_AR antagonist bicuculline was the most potent blocker of the $\alpha 1\beta 3\gamma 2$ isoform that we studied. However, it failed to completely reduce the fluorescence to that in GABA_AR-null cells, a result fully in accord with previous voltage-clamp studies where high concentrations of bicuculline fully block GABA activated Cl⁻ current but not barbiturate-activated current (Rho et al., 1996). Interestingly, bicuculline exhibited the opposite relative selectivity to that of TBPS and fipronil inasmuch as the $\alpha 4\beta 3\delta$ isoform was less sensitive than the $\alpha 1\beta 3\gamma 2$ isoform.

The FMP-Red-Dye potentiometric assay proved to be an excellent system for characterizing both the directly activating and the PAM effects of NAS. Of 20 NAS tested, only 8 activated GABA_AR with potencies (EC₅₀ values) below 1 μ M (**Table 2**). In general, the SAR that emerges from the FMP-Red-Dye assay is consistent with previous reports in the literature (Kokate et al., 1994; Akk et al., 2007; Borowicz et al., 2011; Wang, 2011; Reddy and Rogawski, 2012). Both synaptic and extrasynaptic GABA_AR subtypes respond to NAS (Bianchi and Macdonald, 2003; Maksay et al., 2000). In general, we found comparable potencies (EC₅₀ values) and efficacies ($\Delta F/F_0$ values) of the active steroids at the synaptic $\alpha 1\beta 3\gamma 2$ isoform and

Mol #108563

the extrasynaptic $\alpha 4\beta 3\delta$ isoform. In contrast to the other active steroids which all had similar maximal efficacies, XJ-42, a pentacyclic analog of allopregnanolone with a 17,18-fused carbonitrile-substituted 6-member carbocyclic ring, had substantially greater efficacy although its potency was in line with that of the other active steroids. This observation indicates that modifications that replace the 17-acetyl group of allopregnanolone can enhance neuroactive steroid efficacy, which may provide therapeutic advantages. In addition to directly activating $GABA_A$ R, at low concentrations, NAS act as PAMs to enhance the action of GABA (Kokate et al., 1994). The FMP-Red-Dye assay is able to demonstrate such an effect as illustrated in **Fig. 9A**, which compares the PAM activity of allopregnanolone and ganaxolone, two exemplary NAS currently under clinical investigation (Reddy and Rogawski, 2012). In experiments with the synaptic $\alpha 1\beta 3\gamma 2$ combination, both steroids exhibit substantial PAM activity in the FMP-Red-Dye assay, with allopregnanolone demonstrating modestly greater potency than ganaxolone. Similar relative potencies are obtained in patch-clamp recordings (**Fig. 9B**; see also, Carter et al., 1997). Because of the heightened sensitivity to GABA due to the influence of FMP-Red-Dye, the PAM activity of NAS was measured in the presence of a low concentration GABA (10 nM), to prevent saturation evident even at 100 nM GABA (**Supplemental Fig. 3**). Under these conditions, the FMP-Red-Dye assay generates EC_{50} and fold-increase values that indicate substantially greater potency and efficacy than obtained with electrophysiological methods, but the relative potencies are consistent with previous reports using receptor binding and electrophysiological methods (Carter et al., 1997).

Conclusion

FMP-Red-Dye based assays provide sensitive and quantitative approaches to investigate functional interactions with $GABA_A$ R subtypes mediated through the GABA site, PAM sites, or

Mol #108563

channel pore sites, and is useful not only for discovery of antiseizure drugs, but also for identifying novel channel blockers of interest to insecticide discovery or biosecurity.

Mol #108563

AUTHORSHIP CONTRIBUTIONS

Participated in research design: A.M.N., S.H., H.W. and I.N.P.

Conducted experiments: A.M.N., B.P., V.S. and S.A.

Contributed new reagents or analytic tools: M.A.R., H.W. and I.N.P.

Performed data analysis: A.M.N., B.P., V.S., H.W. and I.N.P.

Wrote or contributed to the writing of the manuscript: A.M.N., B.P., V.S., S.A., S.H., M.A.R.,
H.W. and I.N.P.

REFERENCES

- Adelsberger H, Brunswieck S and Dudel J (1998) Block by picrotoxin of a GABAergic chloride channel expressed on crayfish muscle after axotomy. *Eur J Neurosci* 10(1): 179-187.
- Akabas MH (2004) GABA_A receptor structure-function studies: a reexamination in light of new acetylcholine receptor structures. *Int Rev Neurobiol* 62: 1-43.
- Akk G, Covey DF, Evers AS, Steinbach JH, Zorumski CF and Mennerick S (2007) Mechanisms of neurosteroid interactions with GABA_A receptors. *Pharmacol Ther* 116(1): 35-57.
- Alvarez LD and Estrin DA (2015) Exploring the molecular basis of neurosteroid binding to the beta3 homopentameric GABA_A receptor. *J Steroid Biochem Mol Biol* 154: 159-167.
- Barnard EA, Skolnick P, Olsen RW, Mohler H, Sieghart W, Biggio G, Braestrup C, Bateson AN and Langer SZ (1998) International Union of Pharmacology. XV. Subtypes of gamma-aminobutyric acid_A receptors: classification on the basis of subunit structure and receptor function. *Pharmacol Rev* 50(2): 291-313.
- Belelli D, Harrison NL, Maguire J, Macdonald RL, Walker MC and Cope DW (2009) Extrasynaptic GABA_A receptors: form, pharmacology, and function. *J Neurosci* 29(41): 12757-12763.
- Belelli D and Lambert JJ (2005) Neurosteroids: endogenous regulators of the GABA_A receptor. *Nat Rev Neurosci* 6(7): 565-575.
- Bettler B and Tiao JY (2006) Molecular diversity, trafficking and subcellular localization of GABA_B receptors. *Pharmacol Ther* 110(3): 533-543.
- Bianchi MT and Macdonald RL (2003) Neurosteroids shift partial agonist activation of GABA_A receptor channels from low- to high-efficacy gating patterns. *J Neurosci* 23(34): 10934-10943.
- Borowicz KK, Piskorska B, Banach M and Czuczwar SJ (2011) Neuroprotective actions of neurosteroids. *Front in endocrinology* 2: 50.
- Braat S and Kooy RF (2015) The GABA_A receptor as a therapeutic target for neurodevelopmental disorders. *Neuron* 86(5): 1119-1130.
- Brickley SG and Mody I (2012) Extrasynaptic GABA_A receptors: their function in the CNS and implications for disease. *Neuron* 73(1): 23-34.
- Brown N, Kerby J, Bonnert TP, Whiting PJ and Wafford KA (2002) Pharmacological characterization of a novel cell line expressing human alpha(4)beta(3)delta GABA_A receptors. *Br J Pharmacol* 136(7): 965-974.
- Campagna-Slater V and Weaver DF (2007) Molecular modelling of the GABA_A ion channel protein. *J Mol Graph Model* 25(5): 721-730.
- Cao Z, Hammock BD, McCoy M, Rogawski MA, Lein PJ and Pessah IN (2012) Tetramethylenedisulfotetramine alters Ca²⁺ dynamics in cultured hippocampal neurons:

Mol #108563

mitigation by NMDA receptor blockade and GABA_A receptor-positive modulation. *Toxicol Sci* 130(2): 362-372.

Carter RB, Wood PL, Wieland S, Hawkinson JE, Belelli D, Lambert JJ, White HS, Wolf HH, Mirsadeghi S, Tahir SH, Bolger MB, Lan NC and Gee KW (1997) Characterization of the anticonvulsant properties of ganaxolone (CCD 1042; 3 α -hydroxy-3 β -methyl-5 α -pregnan-20-one), a selective, high-affinity, steroid modulator of the γ -aminobutyric acid_A receptor. *J Pharmacol Exp Ther* 280(3): 1284-1295.

Casida JE and Durkin KA (2015) Novel GABA receptor pesticide targets. *Pestic Biochem Physiol* 121: 22-30.

Chen L, Durkin KA and Casida JE (2006) Structural model for gamma-aminobutyric acid receptor noncompetitive antagonist binding: widely diverse structures fit the same site. *Proc Natl Acad Sci USA* 103(13): 5185-5190.

Chen ZW, Manion B, Townsend RR, Reichert DE, Covey DF, Steinbach JH, Sieghart W, Fuchs K, Evers AS. Neurosteroid analog photolabeling of a site in the third transmembrane domain of the β 3 subunit of the GABA_A receptor. *Mol Pharmacol*. 2012 Sep;82(3):408-19.

Covey DF and Jiang X (2014) Neuroactive 13,24-cyclo-18,21-dinorcholanes and structurally related pentacyclic steroids. US Patent 8,759,330 (Jun. 24, 2014).

Dasheiff RM (1985) A new method of monitoring membrane potential in rat hippocampal slices using cyanine voltage-sensitive dyes. *J Neurosci Methods* 13(3-4): 199-212.

Fairless R, Beck A, Kravchenko M, Williams SK, Wissenbach U, Diem R and Cavalie A (2013) Membrane potential measurements of isolated neurons using a voltage-sensitive dye. *PLoS one* 8(3): e58260.

Herd MB, Belelli D and Lambert JJ (2007) Neurosteroid modulation of synaptic and extrasynaptic GABA_A receptors. *Pharmacol Ther* 116(1): 20-34.

Hogenkamp DJ, Tran MB, Yoshimura RF, Johnstone TB, Kanner R, Gee KW (2014) Pharmacological profile of a 17 β -heteroaryl-substituted neuroactive steroid. *Psychopharmacology (Berl)* 231(17):3517-24.

Hosie AM, Wilkins ME and Smart TG (2007) Neurosteroid binding sites on GABA_A receptors. *Pharmacol Ther* 116(1): 7-19.

Joesch C, Guevarra E, Parel SP, Bergner A, Zbinden P, Konrad D and Albrecht H (2008) Use of FLIPR membrane potential dyes for validation of high-throughput screening with the FLIPR and microARCS technologies: identification of ion channel modulators acting on the GABA_A receptor. *J Biomol Screen* 13(3): 218-228.

Kokate TG, Svensson BE and Rogawski MA (1994) Anticonvulsant activity of neurosteroids: correlation with γ -aminobutyric acid-evoked chloride current potentiation. *J Pharmacol Exp Ther* 270:1223-1229.

Mol #108563

- Löscher W and Rogawski MA (2012) How theories evolved concerning the mechanism of action of barbiturates. *Epilepsia* 53 Suppl 8: 12-25.
- Maksay G, Thompson SA and Wafford KA (2000) Allosteric modulators affect the efficacy of partial agonists for recombinant GABA_A receptors. *Br J Pharmacol* 129(8): 1794-1800.
- McCartney MR, Deeb TZ, Henderson TN and Hales TG (2007) Tonicly active GABA_A receptors in hippocampal pyramidal neurons exhibit constitutive GABA-independent gating. *Mol Pharmacol* 71(2): 539-548.
- Mennerick S, Chisari M, Shu HJ, Taylor A, Vasek M, Eisenman LN and Zorumski CF (2010) Diverse voltage-sensitive dyes modulate GABA_A receptor function. *J Neurosci* 30(8): 2871-2879.
- Miller PS and Aricescu AR (2014) Crystal structure of a human GABA_A receptor. *Nature* 512(7514):270-275.
- Mortensen M, Patel B and Smart TG (2011) GABA Potency at GABA_A Receptors Found in Synaptic and Extrasynaptic Zones. *Front Cell Neurosci* 6: 1.
- Olsen RW (2006) Picrotoxin-like channel blockers of GABA_A receptors. *Proc Natl Acad Sci USA* 103(16): 6081-6082.
- Reddy DS and Rogawski MA (2012) Neurosteroids — Endogenous Regulators of Seizure Susceptibility and Role in the Treatment of Epilepsy. In: Noebels JL, Avoli M, Rogawski MA, Olsen RW and Delgado-Escueta AV, eds. *Jasper's Basic Mechanisms of the Epilepsies* [Internet]. 4th edition. Bethesda (MD): National Center for Biotechnology Information (US). Available from: <https://www.ncbi.nlm.nih.gov/books/NBK98218/>
- Rho JM, Donevan SD and Rogawski MA (1996) Direct activation of GABA_A receptors by barbiturates in cultured rat hippocampal neurons. *J Physiol* 497 (Pt 2):509-522.
- Rissman RA and Mobley WC (2011) Implications for treatment: GABA_A receptors in aging, Down syndrome and Alzheimer's disease. *J Neurochem* 117(4): 613-622.
- Rogawski MA, Löscher W and Rho JM (2016) Mechanisms of action of antiseizure drugs and the ketogenic diet. *Cold Spring Harb Perspect Med.* 6(5). pii: a022780.
- Rudolph U and Möhler H (2014) GABA_A receptor subtypes: Therapeutic potential in Down syndrome, affective disorders, schizophrenia, and autism. *Annu Rev Pharmacol Toxicol* 54: 483-507.
- Sieghart W (1995) Structure and pharmacology of gamma-aminobutyric acid_A receptor subtypes. *Pharmacol Rev* 47(2): 181-234.
- Stafstrom CE, Hagerman P and Pessah IN (2012) Pathophysiology of Epilepsy in Autism Spectrum Disorders. In: Noebels JL, Avoli M, Rogawski MA, Olsen RW and Delgado-Escueta AV, eds. *Jasper's Basic Mechanisms of the Epilepsies* [Internet]. 4th edition. Bethesda (MD): National Center for Biotechnology Information (US). Available from: <https://www.ncbi.nlm.nih.gov/books/NBK98169/>

Mol #108563

- Steinbach JH and Akk G (2001) Modulation of GABA_A receptor channel gating by pentobarbital. *J Physiol* 537(Pt 3): 715-733.
- Verkman AS and Galiotta LJ (2009) Chloride channels as drug targets. *Nat Rev Drug Discov* 8(2): 153-171.
- Wang M (2011) Neurosteroids and GABA-A Receptor Function. *Front Endocrinol (Lausanne)* 2: 44.
- Wooltorton JR, Moss SJ and Smart TG (1997) Pharmacological and physiological characterization of murine homomeric beta3 GABA_A receptors. *Eur J Neurosci* 9(11): 2225-2235.
- Zhao C, Hwang SH, Buchholz BA, Carpenter TS, Lightstone FC, Yang J, Hammock BD and Casida JE (2014) GABA_A receptor target of tetramethylenedisulfotetramine. *Proc Natl Acad Sci USA* 111(23): 8607-8612.

Mol #108563

FOOTNOTES

This work was sponsored by the National Institutes of Health National Institute of Neurological Disorders and Stroke [UC Davis CounterACT Center of Excellence Grant U54 NS 011269] and IDDRRC Core Center [Grant U54 HD079125]; B.P. was supported by a NIGMS-funded Pharmacology Training Program [T32GM099608].

FIGURE LEGENDS

Figure 1. FMP-Red-Dye modulates $\alpha 1\beta 3\gamma 2$ and $\alpha 4\beta 3\delta$ GABA_A receptors expressed in HEK 293 and L-tk cells, respectively. (A, B) FMP-Red-Dye causes a slow increase in fluorescence (AFU) in cells expressing both receptor types over a 30 min period that is blocked by 1 μ M PTX. AFU in GABA_AR-null cells minimally changes during the 30 min after onset of FMP-Red-Dye exposure. (C, D) 1 μ M GABA causes an instantaneous increase in AFU in cells expressing both receptors types compared to GABA_AR-null cells; AFU continues to slowly rise over 30 min. GABA has no effect on AFU in GABA_AR-null cells.

Figure 2. Current clamp experiments demonstrating that incubation with FMP-Red-Dye leads to a depolarization of GABA_AR expressing cells. Membrane potential (V_m) values of $\alpha 1\beta 3\gamma 2$ expressing HEK 293 cells and GABA_AR-null HEK 293 cells measured by current clamp under three conditions: 1) no treatment; 2) incubation with FMP-Red-Dye for 30 min prior to recording membrane potential in the absence or presence of 50 μ M fipronil (FIP); 3) incubation with FMP-Red-Dye for 30 min followed by 10 min of UV irradiation prior to recording membrane potential. $n = 8-10$ cells per condition. Unpaired t-test was used to compare the treatments with control (white bar). * = $P < 0.05$, ** = $P < 0.01$. Each bar represents mean \pm S.D.

Figure 3. Comparison of GABA responses in cells expressing GABA_AR as assessed with the FMP-Red-Dye technique and by voltage-clamp recording. (A) Both $\alpha 1\beta 3\gamma 2$ and $\alpha 4\beta 3\delta$ GABA_AR expressing cells exhibit fluorescence responses of increasing amplitude following exposure to increasing concentrations of GABA in the range 0.1 nM to 30 μ M. In these experiments, cells were equilibrated with FMP-Red-Dye for 30 min. Then, baseline fluorescence was recorded for 2 min followed by exposure to vehicle (VEH; 0.01% DMSO) or GABA. $\Delta F/F_0$ values were determined at the peak of the fluorescence response. The black arrow indicates the time of GABA addition; GABA remained for the duration of the recording. GABA_AR-null cells do not respond to GABA. (B, left) Concentration-response curves for GABA based on fluorescence responses reveals that $\alpha 4\beta 3\delta$ GABA_AR expressed in L-tk cells are significantly more sensitive to GABA than $\alpha 1\beta 3\gamma 2$ GABA_AR expressed in HEK 293 cells [EC_{50} values, 6 nM (95% CI: 4-8 nM) ($n_H = 0.7$; $n=10$) and 40 nM (95% CI: 33-54 nM) ($n_H = 1.1$; $n=10$). $\beta 3$ homopentamers transiently expressed in HEK 293 cell are largely insensitive to GABA ($EC_{50} > 1$ mM). Dose-response curves were plotted using nonlinear regression with a four-parameter logistic equation and independent F test was applied to determine the statistical differences for EC_{50} values and slopes between $\alpha 1\beta 3\gamma 2$ and $\alpha 4\beta 3\delta$ GABA_AR expressing cell lines. Each data point represents mean \pm S.D. of data from

Mol #108563

10 wells. **(B, right)** Concentration-response curves for GABA activation of $\alpha 1\beta 3\gamma 2$ receptors in HEK 293 cells and $\alpha 4\beta 3\delta$ receptors in L-tk cells from whole-cell voltage-clamp recordings [EC_{50} values are 6.67 μM (95% CI: 5.30-8.04 μM , $n_H = 1.8$; $n=13$) and 549 (95% CI: 435-663 nM, $n_H = 1.8$; $n=10$) *], Each data point represents mean \pm S.D. $P < 0.0001$ for $\alpha 1\beta 3\gamma 2$ versus $\alpha 4\beta 3\delta$].

Figure 4. PicROTOXIN (PTX) and TETS block $\alpha 1\beta 3\gamma 2$ GABA_AR-dependent FMP-Red-Dye fluorescence. HEK 293 cells stably transfected with $\alpha 1\beta 3\gamma 2$ GABA_AR were exposed to FMP-Red-Dye for 30 min to activate the receptors. GABA_AR-null cells were used as control. PTX **(A)** or TETS **(C)** caused a slow, concentration-dependent inhibition of the fluorescence in cells expressing $\alpha 1\beta 3\gamma 2$ GABA_AR; minimal effects were obtain in GABA_AR-null cells. Arrows indicate time of addition of PTX and TETS to the wells; the blockers were not removed. **(B, D)** Plots of $\Delta F/F_0$ from experiments similar to those illustrated in (A, C). Each plot represents 8 experiments. IC_{50} values are 6.5 μM (95% CI: 3.2-12 μM) and 3.8 μM (95% CI: 2.8-5.2 μM) for PTX and TETS, respectively. TETS is significantly more potent than PTX ($P < 0.0001$). Dose-response curves were plotted using nonlinear regression with a four-parameter logistic equation and independent F test was applied to determine the statistical differences for EC_{50} values between TETS and PTX. Each data point represents mean \pm S.D. of data from 8 wells. Red traces represent responses to vehicle (0.01% DMSO). * $P < 0.0001$.

Figure 5. GABA potentiation and PTX inhibition of $\beta 3$ homopentameric GABA_AR-dependent FMP-Red-Dye fluorescence. HEK 293 cells transiently transfected with $\beta 3$ homopentameric GABA_AR were exposed to FMP-Red-Dye for 30 min to activate the receptors. GABA_AR-null cells were used as control. **(A)** GABA caused a slow, concentration-dependent potentiation of the fluorescence in cells expressing $\beta 3$ homopentameric GABA_AR; minimal effects were obtained in GABA_AR-null cells. **(B)** PTX caused a slow, concentration-dependent inhibition of the fluorescence in cells expressing $\beta 3$ homopentameric GABA_AR; minimal effects were obtained in GABA_AR-null cells. Arrows indicate time of addition of GABA and PTX, which was not removed. Red traces represents the responses to vehicle (0.01% DMSO). **(B, D)** Plots of $\Delta F/F_0$ from experiments similar to those illustrated in (A, C). Each data point represents mean \pm S.D. of data from 10 wells. EC_{50} value for GABA could not be determined as the response did not plateau. IC_{50} value for PTX is 1.8 μM (95% CI: 1.4-2.2 μM). Dose-response curves were plotted for PTX using nonlinear regression with a four-parameter logistic equation.

Figure 6. Fipronil blocks $\beta 3$ -homomeric GABA_A receptors, while allpregnanolone fails to affect the fluorescence signal even at concentrations $\geq 10 \mu M$. **(A)** Fipronil blocks $\beta 3$ receptors in a concentration-dependent manner, but does not have any significant effects on GABA_AR-null cells. Dose-response curves were plotted using nonlinear regression with a four-parameter logistic equation. Each data point

Mol #108563

represents mean \pm S.D. of data from 8 wells. **(B)** Allopregnanolone, does not have any effect even at 10 μ M.

Figure 7. Neuroactive steroid-induced FMP-Red-Dye fluorescence responses of $\alpha_1\beta_3\gamma_2$ GABA_AR in HEK 293 cells. **(A, B, C & D)** Representative traces of responses to 0.01 nM to 10 μ M of eltanolone, allopregnanolone, XJ-42 and ganaxolone, respectively. Arrow indicates time of addition of the test compound, which was not removed. Red traces represent the responses to vehicle (0.01% DMSO). **(E)** Concentration-response curves for each of the neuroactive steroids and cortisol. Dose-response curves were plotted using nonlinear regression with a four-parameter logistic equation. Separate one way anova with additional correction (Tukey) for post-hoc multiple comparison was applied for EC₅₀ and slope to determine the statistical differences within a subunit composition –not across subtypes (Table 2). Each data point represents mean \pm S.D. of data from 10 wells.* P value <0.0001

Figure 8. Neuroactive steroid-induced FMP-Red-Dye fluorescence responses of $\alpha_4\beta_3\delta$ GABA_A receptors in L-tk cells. **(A, B, C & D)** Representative traces of responses to 0.01 nM to 10 μ M of eltanolone, allopregnanolone, XJ-42 and ganaxolone, respectively. Arrow indicates time of addition of test compound, which was not removed. Red traces represent the responses to vehicle (0.01% DMSO). **(E)** Concentration-response curves for each of the neuroactive steroids. Dose-response curves were plotted using nonlinear regression with a four-parameter logistic equation. Separate one way anova with additional correction (Tukey) for post-hoc multiple comparison was applied for EC₅₀ and slope to determine the statistical differences within a subunit composition –not across subtypes (Table 2). Each data point represents mean \pm S.D. of data from 10 wells.* P value <0.0001

Figure 9. Allopregnanolone and ganaxolone potentiation of GABA responses of $\alpha_1\beta_3\gamma_2$ GABA_AR in HEK 293 cells. **(A)** Concentration-response curves for allopregnanolone and ganaxolone potentiation of FMP-red dye responses to 10 nM GABA. The graph plots mean \pm S.D. fold increase in peak response in the presence the neuroactive steroid compared with the response to 10 nM GABA alone. Each data point is the mean \pm S.D. of measurements of 10 wells. EC₅₀ values for allopregnanolone and ganaxolone are 1.7 nM (95% CI: 1-3.1 nM, $n_H = 1.5$) and 20 nM (95% CI: 14-55 nM, $n_H = 1.4$), respectively (P < 0.0001). Dose-response curves were plotted using nonlinear regression with a four-parameter logistic equation and independent F test was applied to determine the statistical differences for EC₅₀ values and slopes between allopregnanolone and ganaxolone in combination with 10 nM GABA in $\alpha_1\beta_3\gamma_2$ GABA_AR in HEK 293 cells. Inset shows representative traces with addition of GABA alone and GABA plus allopregnanolone at concentrations of 1 nM and 10 nM. **(B)** Concentration-response curves for allopregnanolone and ganaxolone potentiation of peak inward Cl⁻ current responses to 1 μ M GABA (EC₁₀ value) in patch-

Mol #108563

clamp recordings. Each data point is the mean \pm S.D. of measurements of 3-6 cells. EC₅₀ values for allopregnanolone and ganaxolone are 71.3 nM (95% CI: 57.1-85.5 nM, $n_H = 1.8$) and 114.8 nM (95% CI: 99.2-130.4 nM, $n_H = 2.2$). Inset shows representative traces with application of GABA alone and GABA plus allopregnanolone at 100 nM and 175 nM.

Figure 10. Effects of midazolam on FMP-Red-Dye fluorescence in cells expressing $\alpha 1\beta 3\gamma 2$ GABA_AR. In the absence of GABA, midazolam fails to generate substantial fluorescence signals compared with vehicle (VEH) except at high concentrations (>1 μ M). GABA (10 nM) induces a small fluorescence signal. Combination of midazolam and GABA results in potentiation of the signal [EC₅₀, 51 nM (95% CI: 30-83 nM)]. Dose-response curves were plotted using nonlinear regression with a four-parameter logistic equation. Each data point represents the mean \pm S.D. of measurements in 8 cells.

Mol #108563

TABLE 1

Potencies of blockers on $\alpha 1\beta 3\gamma 2$, $\alpha 4\beta 3\delta$ and $\beta 3$ homopentamer GABA_AR isoforms as assessed using the FMP-Red-Dye fluorescence assay

$\alpha 1\beta 3\gamma 2$					
	PTX	TETS	TBPS	Fipronil	Bicuculline
IC₅₀ (95% CI)	6.5 μ M * (3.2 - 12 μ M)	3.8 μ M (2.8 - 5.2 μ M)	1.8 μ M (1.1 - 2.9 μ M)	2.6 μ M (1.6 - 3.6 μ M)	0.1 μ M * (0.03 - 0.8)
Slope (95% CI)	-1.0 (-1.7 to -0.1)	-1.8 (-2.6 to -0.9)	-0.7 * (-0.8 to -0.5)	-0.8 (-1 to -0.7)	-1 (-1.4 to -0.3)
$\alpha 4\beta 3\delta$					
	PTX	TETS	TBPS	Fipronil	Bicuculline
IC₅₀	6 μ M (2.9 - 13 μ M)	7 μ M (4 - 15 μ M)	0.01 μ M * (0.009 - 0.015 μ M)	0.25 μ M * (0.14 - 0.5 μ M)	7 μ M (6.8 to 9 μ M)
Slope	-0.1 (-0.2 to -0.07)	-0.1 (-0.3 to -0.04)	-1 * (-1.2 to -0.7)	-0.40 * (-0.7 to -0.1)	-1 * (-1.5 to -0.5)
$\beta 3$ homopentamer					
	PTX	TETS	TBPS	Fipronil	Bicuculline
IC₅₀	1.8 μ M * (1.4 - 2.2 μ M)	10 μ M (8.6 - 11 μ M)	Not tested	0.2 μ M * (0.1 - 0.9 μ M)	Not tested
Slope	-1.7 (-2.2 to -1.2)	-2.1 (-2.7 to -1.4)	Not tested	-0.6 * (-0.8 to -0.3)	Not tested

Dose-response curves were plotted using nonlinear regression with a four-parameter logistic equation. Separate one way anova with additional correction (Tukey) for post-hoc multiple comparison was applied for EC₅₀ and slope to determine the statistical differences among them. IC₅₀ values and slopes were compared within each receptor isoform. On $\alpha 1\beta 3\gamma 2$ GABA_A receptors bicuculline is significantly more potent than the other blockers; the IC₅₀ values of the other blockers were not significantly different from each other. On $\alpha 4\beta 3\delta$ GABA_A receptors, TBPS and fipronil are significantly more potent than the other blockers. The slope values for PTX and TETS are significantly smaller than for the other blockers. On $\beta 3$ homopentamer, fipronil is more potent than PTX and TETS. The slope for fipronil is significantly smaller than that of PTX and TETS. Each data point represents the mean (with 95% confidence interval in parenthesis) of measurements in 8 wells. * P value <0.001 when comparing IC₅₀ values or slopes of blockers within each receptor isoform.

Mol #108563

TABLE 2

EC₅₀ and maximum ΔF/F₀ values (95% confidence interval in the parenthesis) for neuroactive steroids and related compounds and benzodiazepines to increase FMP-Red-Dye fluorescence in cells expressing α1β3γ2 and α4β3δ GABA_AR in the absence of GABA

Compound Common Name (Systematic Name)	α1β3γ2		α4β3δ	
	EC ₅₀ (95% CI)	Maximum ΔF/F ₀ (95% CI)	EC ₅₀ (95% CI)	Maximum ΔF/F ₀ (95% CI)
Allopregnanolone (3α-hydroxy-5α-pregnan-20-one)	9 nM * (7 - 11 nM)	0.13 (0.12 - 0.13)	27 nM (18 - 42 nM)	0.16 (0.15 - 0.17)
Ganaxolone (3α-hydroxy-3β-methyl-5α-pregnan-20-one)	24 nM (18 - 32 nM)	0.14 (0.13 - 0.14)	40 nM (21 - 73 nM)	0.17 (0.15 - 0.18)
Eltanolone (3α-hydroxy-5β-pregnan-20-one)	8 nM * (5 - 14 nM)	0.17 * (0.16 - 0.18)	6 nM * (2.4 - 16 nM)	0.14 (0.12 - 0.15)
XJ-42 (3α,5α,20E)-3-hydroxy-13,24-cyclo-18-norcholan-20-ene-21-carbonitrile)	11 nM * (7 - 17 nM)	0.13 (0.12 - 0.14)	74 nM (47 - 116 nM)	0.41 * (0.38 - 0.45)
5β,3α-THDOC (5β-pregnan-3α,21-diol-20-one)	16 nM (6 - 45 nM)	0.09 (0.08 - 0.10)	54 nM (12 - 230 nM)	0.09 (0.06 - 0.12)
Alphadolone 21-acetate (5α-pregnan-3α,21-diol-11, 20-dione 21-acetate)	60 nM (33 - 100 nM)	0.08 (0.07 - 0.09)	700 nM (381 - 1220 nM)	0.14 (0.1 - 0.18)
Alphaxalone (3α,5α)-3-hydroxypregnane-11,20-dione)	26 nM (13 - 54 nM)	0.11 (0.10 - 0.11)	83 nM (72 - 97 nM)	0.13 (0.11 - 0.15)
Androsterone (5α-androstan-3α-ol-17-one)	300 nM (200 - 551 nM)	0.16 * (0.14 - 0.18)	> 1 μM	
Etiocholanolone (5β-androstan-3α-ol-17-one)	> 1 μM		> 5 μM	
Org 20599 (2β,3α,5α)-21-chloro-3-hydroxy-2-(4-morpholinyl)pregnan-20-one)	> 1 μM		> 1 μM	
UCI-50027 (3-[3α-hydroxy-3β-methyl-5α-androstan-17β-yl]-5(hydroxymethyl)isoxazole)	> 5 μM		> 5 μM	
Progesterone (pregn-4-ene-3,20-dione)	> 5 μM		> 5 μM	
Epiandrosterone (5α-androstan-3β-ol-17-one)	> 5 μM		> 5 μM	
Indiplon (N-methyl-N-[3-[3-(2-thienylcarbonyl)pyrazolo[1,5-a]pyrimidin-7-yl]phenyl]-acetamide)	> 5 μM		> 5 μM	
Androstenediol (5-Androsten-3β, 17β-diol)	> 5 μM		> 5 μM	
Dehydroepiandrosterone (DHEA) acetate	> 5 μM		> 10 μM	
Dehydroepiandrosterone (DHEA)	> 5 μM		Inactive	
20α-Dihydropregnenolone (5-pregnen-3β,20α-diol)	> 10 μM		> 10 μM	
Ursodeoxycholic Acid (sodium salt) (3,7-dihydroxy-cholan-24-oic acid, monosodium salt)	Inactive		Inactive	
Cortisol (4-pregnen-11β,17,21-triol-3,20-dione)	Inactive		Inactive	
Diazepam (7-Chloro-1-methyl-5-phenyl-1,3-dihydro-2H-1,4-benzodiazepin-2-one)	> 10 μM		> 10 μM	
Midazolam (8-Chloro-6-(2-fluorophenyl)-1-methyl-4H-imidazo[1,5-a][1,4]benzodiazepine)	> 10 μM		> 10 μM	
Zolpidem (N,N,6-trimethyl-2-(4-methylphenyl)-imidazo[1,2-a]pyridine-3-acetamide)	> 10 μM		> 10 μM	

Mol #108563

In Table 2, dose-response curves were fit by nonlinear regression with a four-parameter logistic equation. Statistical differences among EC_{50} and maximum $\Delta F/F_0$ values were assessed independently by one-way ANOVA with post-hoc pairwise comparisons using Tukey's HSD test. On $\alpha 1\beta 3\gamma 2$ GABAA receptors eltanolone with IC_{50} value of 8 nM and maximum of 0.17 is the most potent and efficacious compound. Although on $\alpha 4\beta 3\delta$ GABAA receptors eltanolone with IC_{50} value of 6 nM is the most potent compound, XJ-42 with maximum of 0.41 is the most efficacious compound. Each data point represents the mean (with 95% confidence interval in parenthesis) of measurements in 10 wells. * P value <0.001 when comparing IC_{50} values or maximum of compounds within each receptor isoform.

Figures

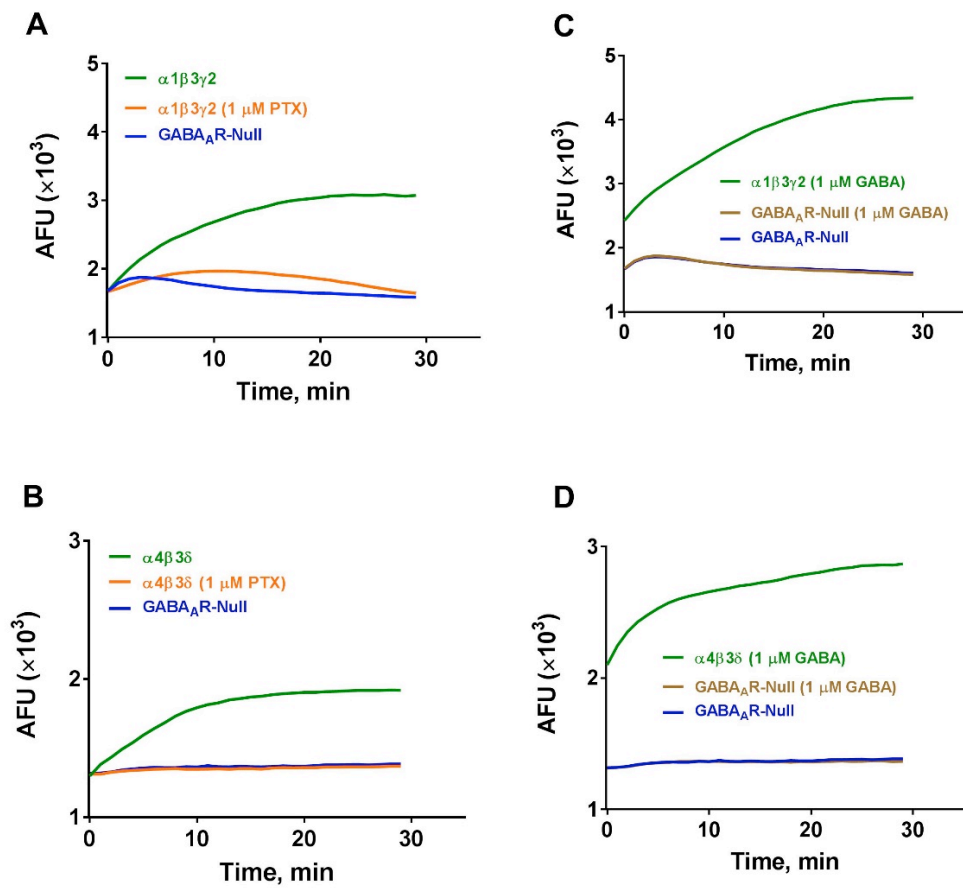


Figure 1

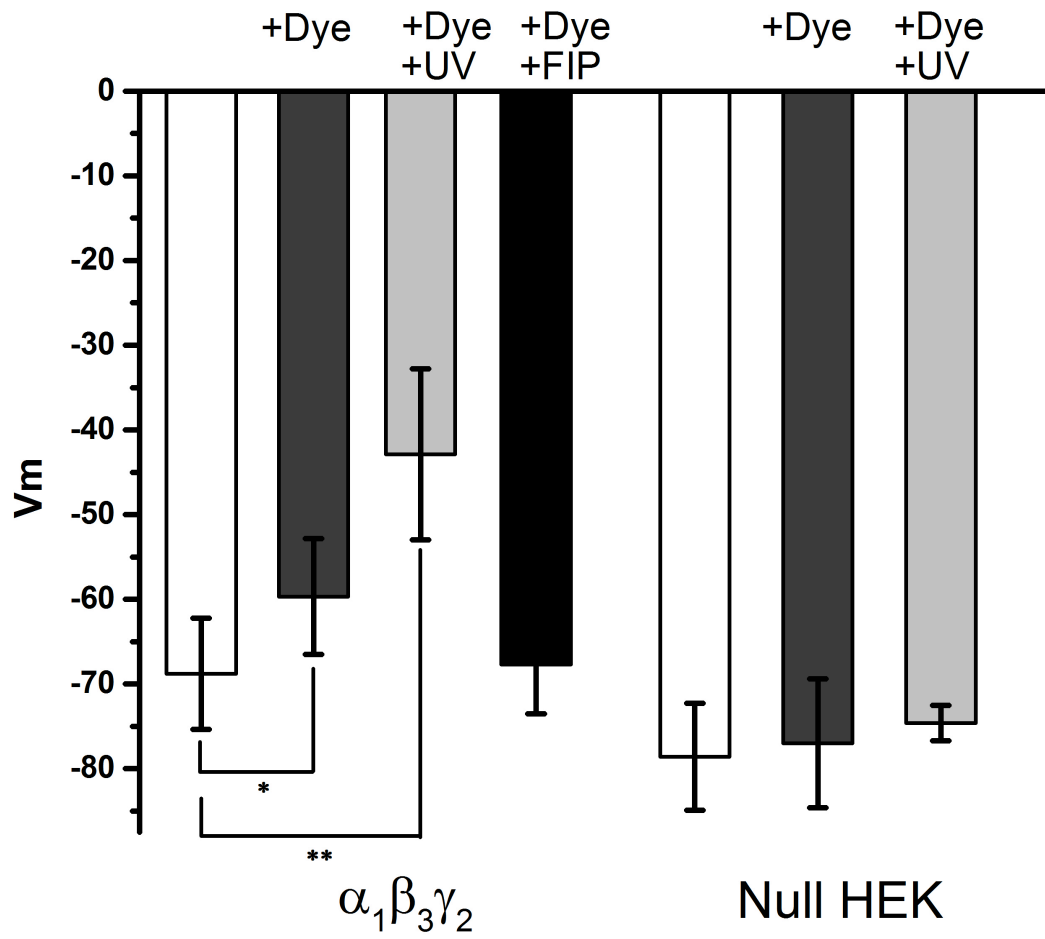


Figure 2

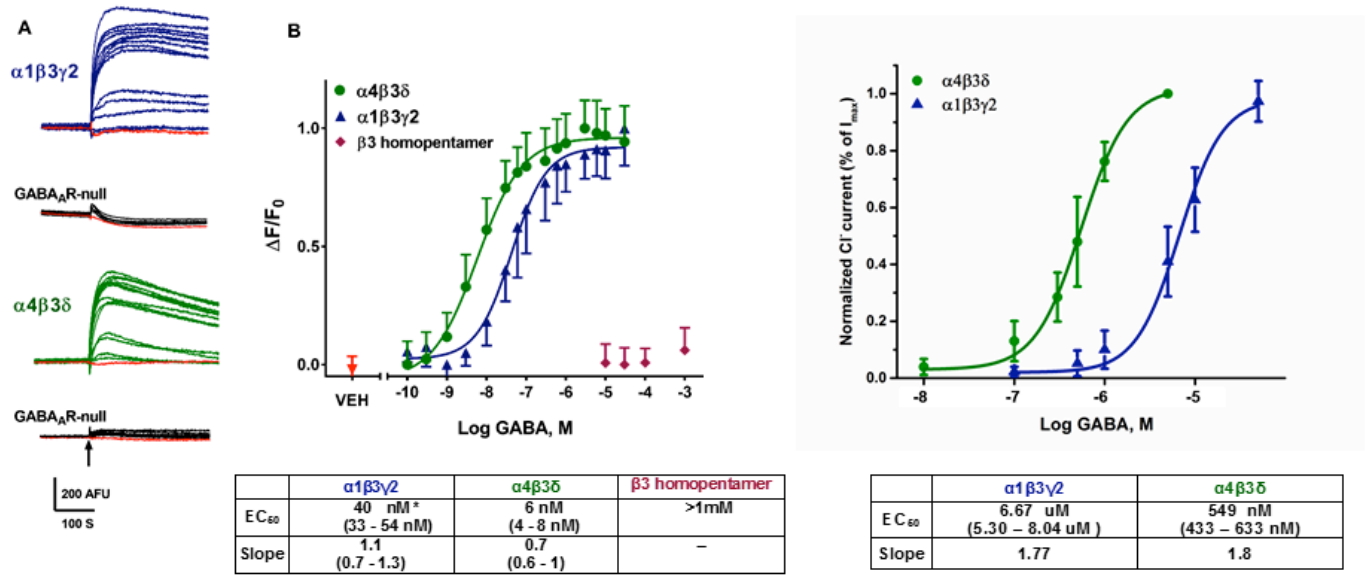


Figure 3

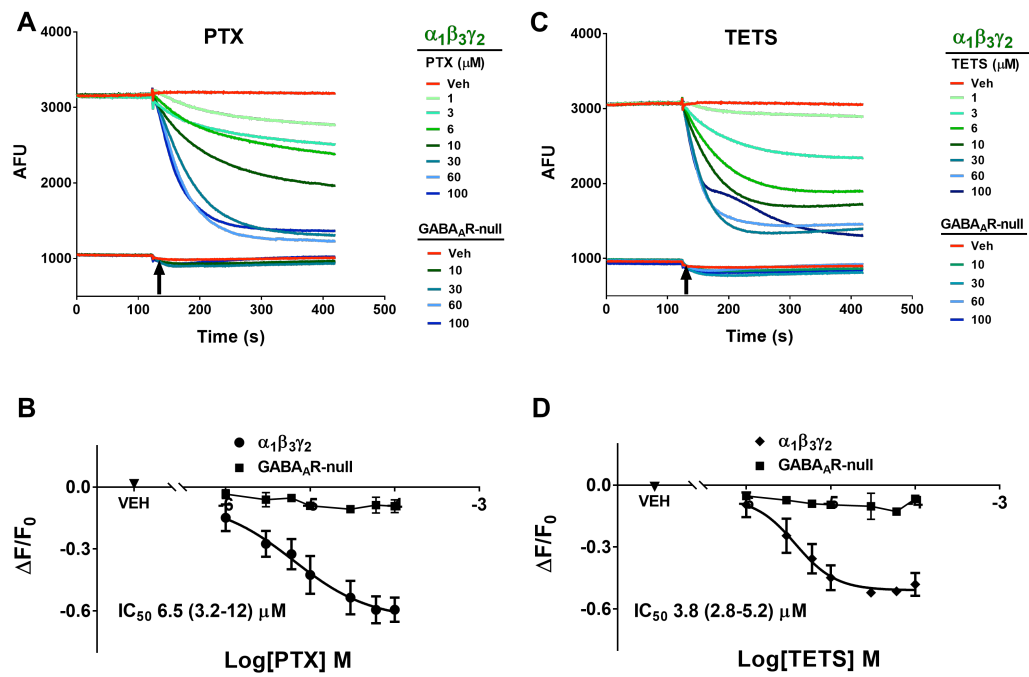


Figure 4

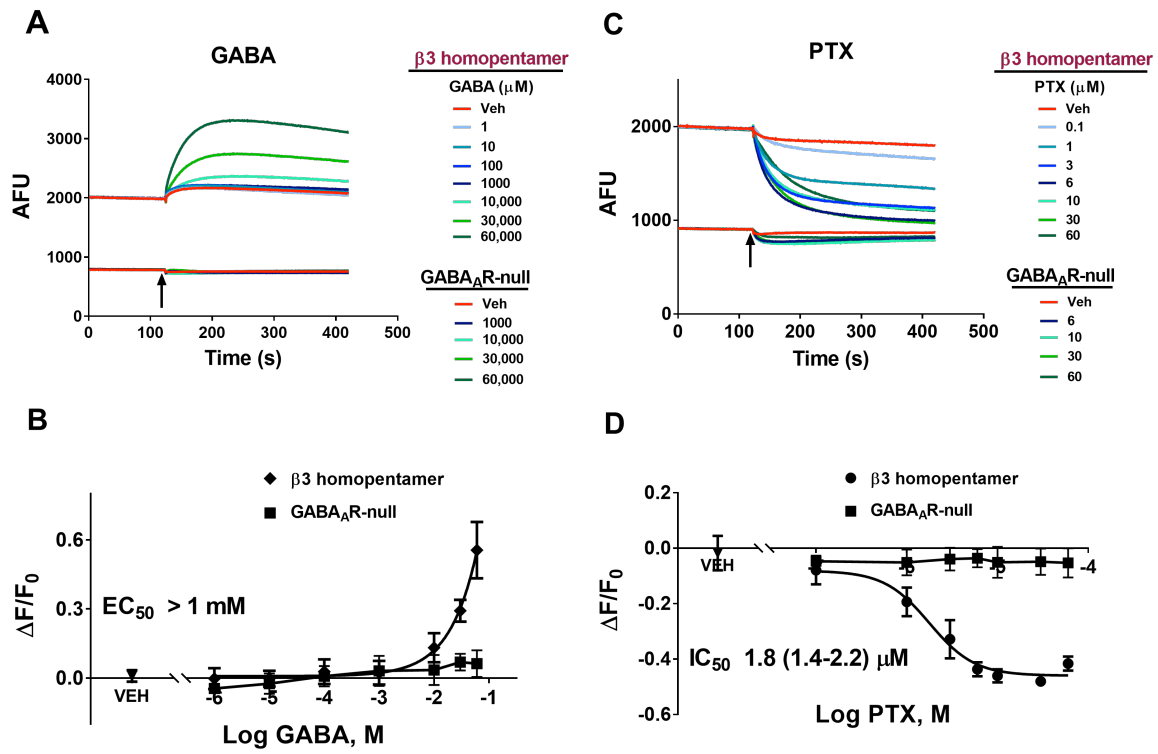


Figure 5

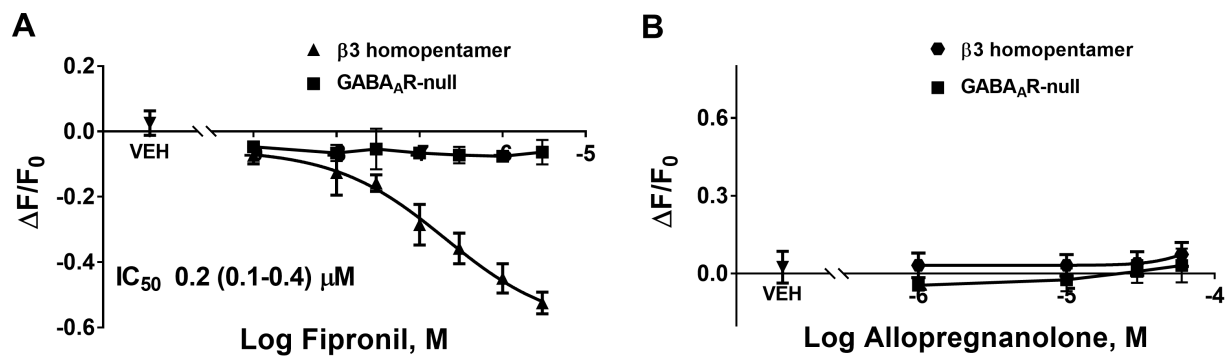


Figure 6

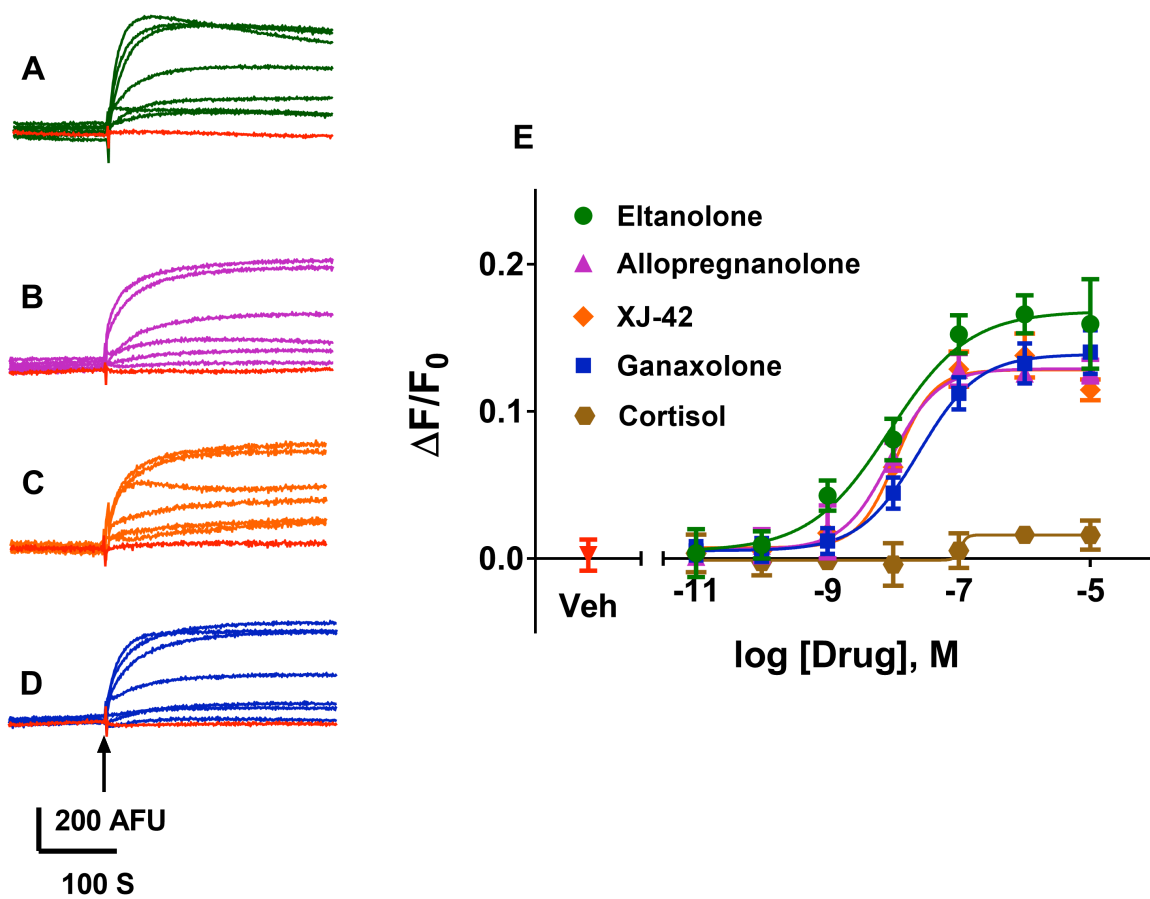


Figure 7

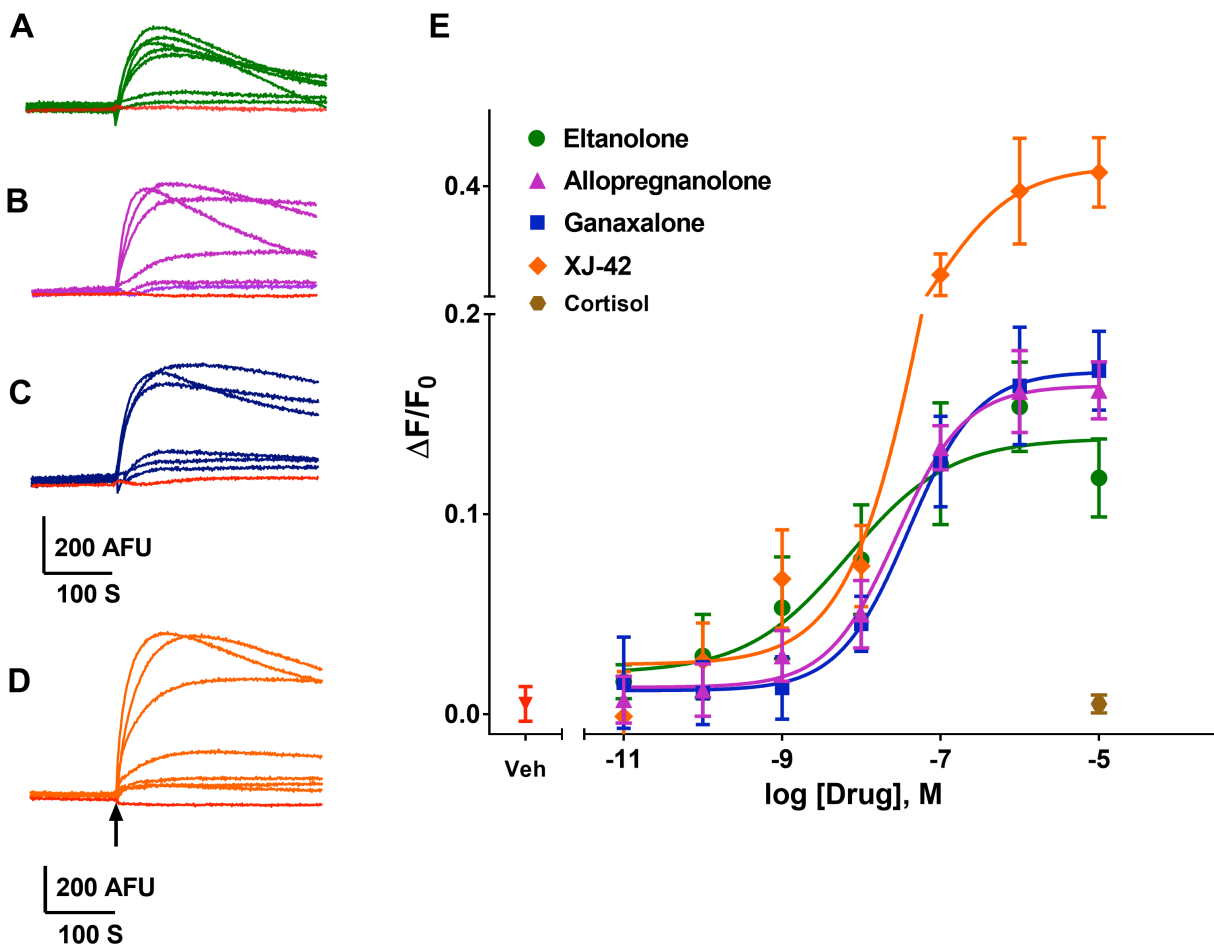


Figure 8

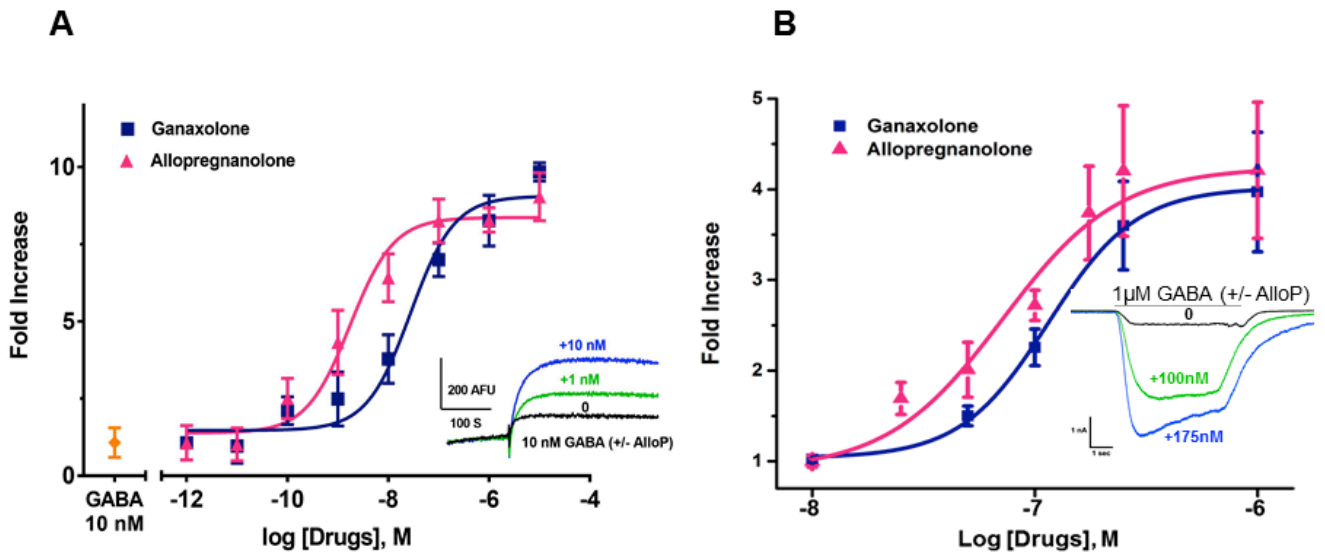


Figure 9

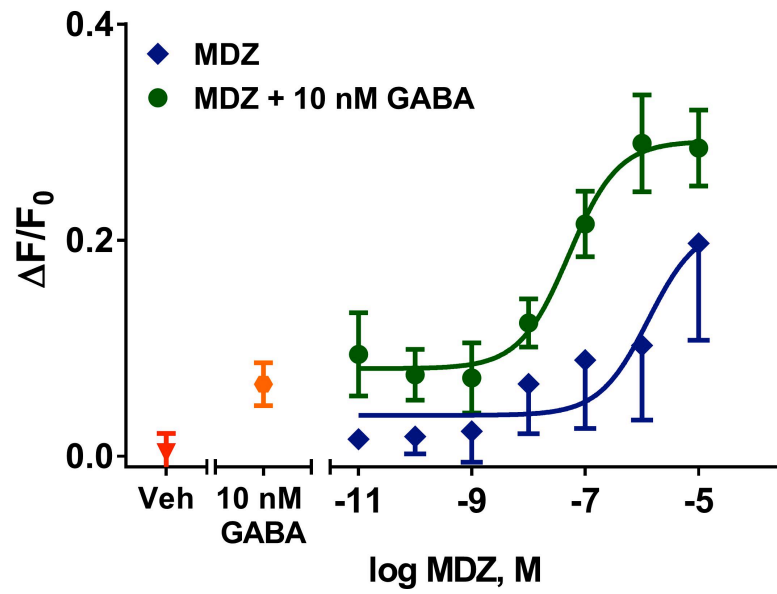


Figure 10